Heterometallic Base Pair Programming in Designer 3D DNA Crystals

Brandon Lu, ¹ Yoel P. Ohayon, ¹ Karol Woloszyn, ¹ Chu-fan Yang, ¹ Jesse B. Yoder, ² Lynn J.

Rothschild, ³ Shalom J. Wind, ⁴ Wayne A. Hendrickson, ⁵ Chengde Mao, ⁶ Nadrian C. Seeman, †¹

James W. Canary, Ruojie Sha, and Simon Vecchioni1*

Abstract

Metal-mediated DNA (mmDNA) is a pathway towards engineering bioinorganic and electronic behavior into DNA devices. Many chemical and biophysical forces drive the programmable chelation of metals between pyrimidine base pairs. Here we develop a crystallographic method using the 3D DNA tensegrity triangle motif to capture single- and multi-metal binding modes across granular steps at environmental pH using anomalous scattering. Leveraging this programmable crystal, we determine 28 biomolecular structures to capture mmDNA reactions. We find that silver(I) binds with increasing occupancy in T-T and U-U pairs at elevated pH levels and exploit this to capture silver(I) and mercury(II) within the same base pair and isolate the titration points for homo- and heterometal base pair modes. We additionally determined the structure of a C-C pair with both silver(I) and mercury(II). Finally, we extend our paradigm to capture cadmium(II) in T-T pairs together with mercury(II) at high pH. The precision self-assembly of heterometallic DNA chemistry at the sub-nanometer scale will enable atomistic design frameworks for more elaborate mmDNA-based nanodevices and nanotechnologies.

Main Text

The predictability of Watson-Crick base pairing has allowed for the construction of a variety of DNA nanostructures.¹⁻⁷ The discovery and design of alternate base pairs, such as the 8-letter

¹Department of Chemistry, New York University, New York, NY 10003, USA.

²IMCA-CAT, Argonne National Lab, Argonne, IL 60439, USA.

³NASA Ames Research Center, Planetary Sciences Branch, Moffett Field, CA 94035, USA.

⁴Department of Applied Math and Applied Physics, Columbia University, New York, NY 10027, USA.

⁵Department of Biochemistry and Molecular Biophysics, Columbia University, New York, NY 10032, USA.

⁶Department of Chemistry, Purdue University, West Lafayette, Indiana 47907, USA.

[†]Deceased

^{*}Correspondence: sv1091@nyu.edu

"Hachimoji" DNA have increased the size and complexity of DNA motif design. 8,9 In this manner, the incorporation of metals into pyrimidine pairs through the two classical examples of dT:Hg²⁺:dT¹⁰ and dC:Ag⁺:dC¹¹ allows for a targeted expansion of the DNA programming language toward the introduction of bioinorganic behavior into DNA motifs that would lead to enhanced electron conduction.¹² These two transition metal ions can selectively fill the gap between two pyrimidine nucleobases at the center N3 position of both nucleobases with a high ion specificity and orthogonality (Figure 1). 10-17 While there have been many instances of metal-mediated DNA (mmDNA) base pair motifs solved through x-ray crystallography^{14-16,18,19} and NMR spectroscopy, 11,17 more datapoints are required to understand the behavior of these complexes in order to advance the use of metal base pairs for structured DNA nanodevices, and to our knowledge, no crystallographic examples yet exist showing both ions in the base pair complex. 12,20,21 There have been a number of exceptions to the "silver binds cytosine and mercury binds thymine" paradigm, such as a non-B-form dT:Ag⁺:dT base pair, ¹⁵ 4-thiothymine binding two silver(I) ions at both the N3 and O4 positions, ¹⁶ and more. ^{19,22-25} This suggests that under certain conditions, uracil family bases (dT, dU, and modified dU) have the ability to bind both silver(I) and mercury(II). In this regard, our current understanding of these metal-DNA interactions remains incomplete. To this end, we have undertaken a systematic structural characterization of mmDNA dynamics using designer 3D crystals.

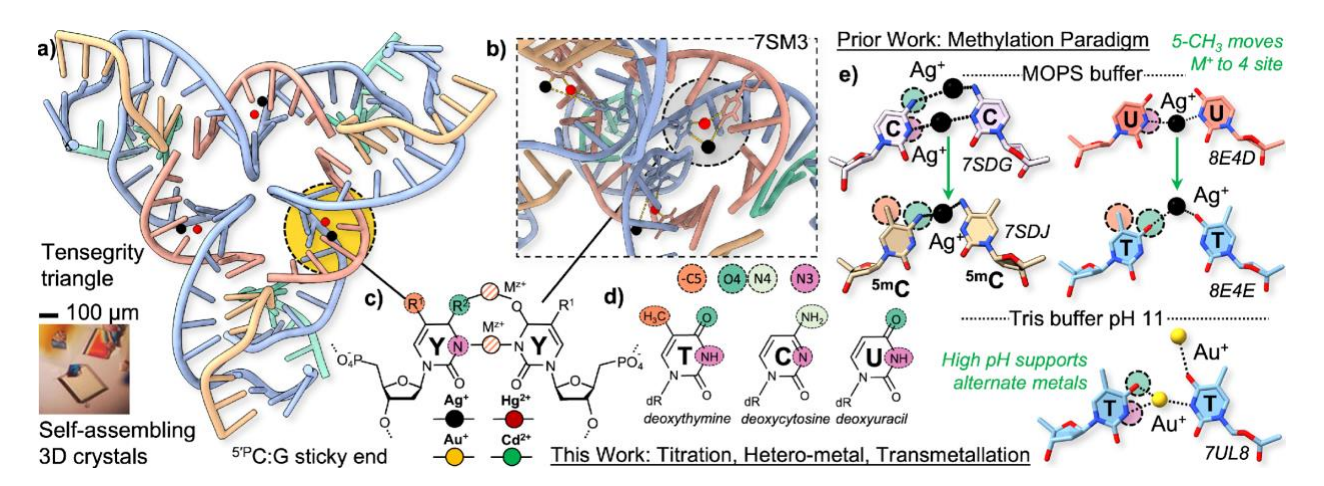


Figure 1. mmDNA binding center used in this study. **a)** The tensegrity triangle is a DNA motif with threefold symmetry that polymerizes into macroscopic crystals through sticky-end cohesion.²⁶ **b)** The center of each triangle edge contains either a dT-dT, dC-dC or dU-dU pair, which can selectively bind Ag⁺ (black spheres) and/or Hg²⁺ ions (red spheres). PDB ID: 7SM3;

 $dT:Hg^{2+}/Ag^+:dT$ at pH 9.0 shown here, which is generalized as a pyrimidine (Y) reaction center—Y:M/M:Y. **c)** Two metal binding sites are described, the N3, centrosymmetric site (pink circle) and the 4-position major groove site (green circle). Here, $R^1 = CH_3$, H; $R^2 = O$, NH₂. **d)** The site-labeled nucleobases used in this study: dT, dC, and dU. **e)** Prior work⁹ determined that methylation of bases at the 5-position causes metals to bind exclusively to the O4 position. High pH allowed for binding metals other than silver and mercury with dT:Au⁺:dT at pH 11.0 (PDB ID: 7UL8).

We make use of the tensegrity triangle motif, which reliably self-assembles into 3D DNA crystals with designed unit cell parameters and space group based on the semantomorphic programming of DNA oligomers (Figure 1a, Figure S1, Table S1). 1,2,9,26-31 Each triangle center contains one mmDNA base pair (Figure 1b) with two possible metal binding sites (Figure 1c), allowing us to test thymine, uracil, and cytosine (Figure 1d). Previously, we found that 5-methylcytosine pairs (PDB ID: 7SDJ) bind silver(I) exclusively at the major groove N4 position, while cytosine pairs exhibit multiple binding sites within a single base pair (Figure 1e). The impact of the electrondonating methyl group at the 5 position suggests that the electronic structure of the nucleobase impacts the coordination of metal ions.³²⁻³⁴ Similar modifications to the 5 position have also generated atypical binding schemes.²² Based on these findings, we hypothesized that solvent pH values, which also impact the electronic structure of nucleobases, 33 would have a major effect on metal coordination to the DNA bases. In this study, we tested these claims by screening dT-dT, dC-dC and dU-dU motifs with silver(I), mercury(II), and other transition metals across a wide range of pH values. The crystal structures we solved here display observable differences in metal identity and occupancy with pH fluctuations and showcased the significant impact of pH on programmable mmDNA structures.

Results and Discussion

pH Titration in dT:Ag+:dT and dU:Ag+:dU

Our prior work determined that dT and dU are capable of binding two silver(I) ions, one at the N3 and one at the O4 site at very high occupancy at neutral pH (**Figure 1e**). We tested these findings using crystallization buffer containing Tris (tris(hydroxymethyl)aminomethane) rather than MOPS (3-(N-morpholino)propanesulfonic acid) and found that (1) Tris buffer results in silver(I) binding exclusively at the O4 position and (2) the pH of the crystallization conditions determined the

occupancy of the silver(I) ion, both properties not found in MOPS. As such, we believed Tris to enable additional specificity of mmDNA base pairing and used Tris in the present study.

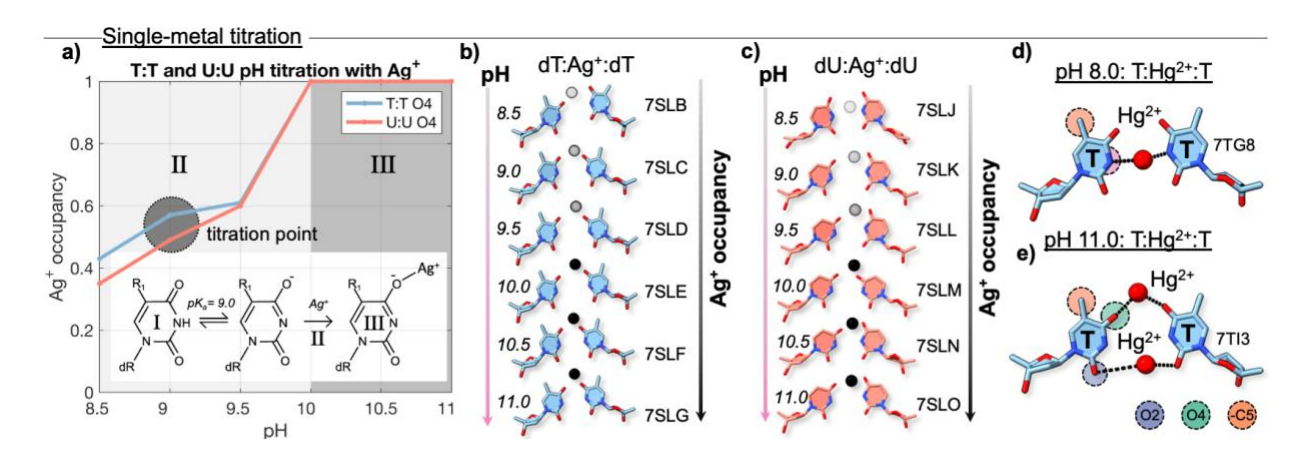


Figure 2: Crystallographic pH titrations for single metal (dT:Ag⁺:dT and dU:Ag⁺:dU) mmDNA base pairs in Tris buffer. **a)** Occupancies of Ag⁺ in dT-dT and dU-dU crystal structures from pH 8.5 to pH 11.0. All ions are found at the O4 position in the major groove, Reaction mechanism drawn for this transition (inset), which begins with the deprotonation of the nitrogen at the N3 position, with a pKa of \sim 9.0. R₁ = H, CH₃, for dU and dT, respectively. **b-c)** Crystal structures of these mmDNA base pairs across pH values, with transparency of Ag⁺ (black sphere) corresponding to normalized occupancy of the ion. pH values and PDB IDs are noted. **d-e)** Structures of dT:Hg²⁺:dT at pH 8.0 and 11.0, respectively.

Motifs containing dT:Ag⁺:dT (**Figure S2**) and dU:Ag⁺:dU (**Figure S3**) were crystallized in buffers of pH 5.0, 5.5, 6.0, 6.5, 7.0, 8.5, 9.0, 9.5, 10.0, 10.5, and 11.0 (**Figure 2a, Table S2**). Only the crystals at pH 8.5 and above were large enough for diffraction analysis (>20 m in length). Crystals were analyzed at beamline APS 17ID (Argonne National Laboratory) at 12307 eV and diffracted to 3.7-4.8 Å (PDB ID: 7LSB-7SLG, 7SLJ-7SLO). Silver was used as a phasing agent and the positions of the silver ions were obtained with anomalous dispersion data. In every crystal structure, the silver(I) ion was located exclusively at the O4 position in the major groove in thymine (**Figure 2b**) and uracil (**Figure 2c**). The lack of an N3-bound silver in any of the crystal structures indicates a departure from prior examples of thymine-bound silver(I), which exhibited N3 binding. The occupancies were plotted at each pH point and a titration curve was obtained (**Figure 2a**). These data confirmed the pH dependence of silver(I) binding in both thymine and uracil pairs, which was hinted in previous studies and showcased the ability for tunable atomistic

control of silver(I) coordination in DNA. In each titration curve, silver(I) occupancy increased with pH and exhibited an inflection point at pH ~9.5, which is close to the N3 pKa values of thymine (9.86) and uracil (9.36).³⁵ As such, we suspect that the pH dependence of silver(I) coordination could be related to the deprotonation at the N3 position, which was previously suggested to be responsible for the binding of mercury(II) to the N3 position.³⁶ A prior study of the binding of zinc(II) to 5-hydroxyuracil showed similarly that basic pH conditions allowed for the deprotonation of the 5-hydroxyl group and thus enabled zinc(II) capture.³⁷ Additionally, the O4 position in deprotonated thymine and uracil was found in prior studies to be a significant hydrogen bond acceptor,³⁸ which may play a role in silver(I) binding to the O4 position. As such, discovery of the pH-dependent O4 position shows that solvent pH not only affects the positions that can be protonated or deprotonated but also targets additional positions *via* resonance by favoring the amide or imine resonance structures of thymine and uracil. A full titration curve was not produced for mercury(II) structures, but we observe that at pH 8.0, there is one mercury(II) ion at the N3 position (Figure 2d), but there are two mercury(II) ions at the O2 and O4 positions at pH 11.0 (Figure 2e), showing possible pH dependence.

Heterobimetallic Chelation of Ag⁺ and Hg²⁺ in a Single Base Pair

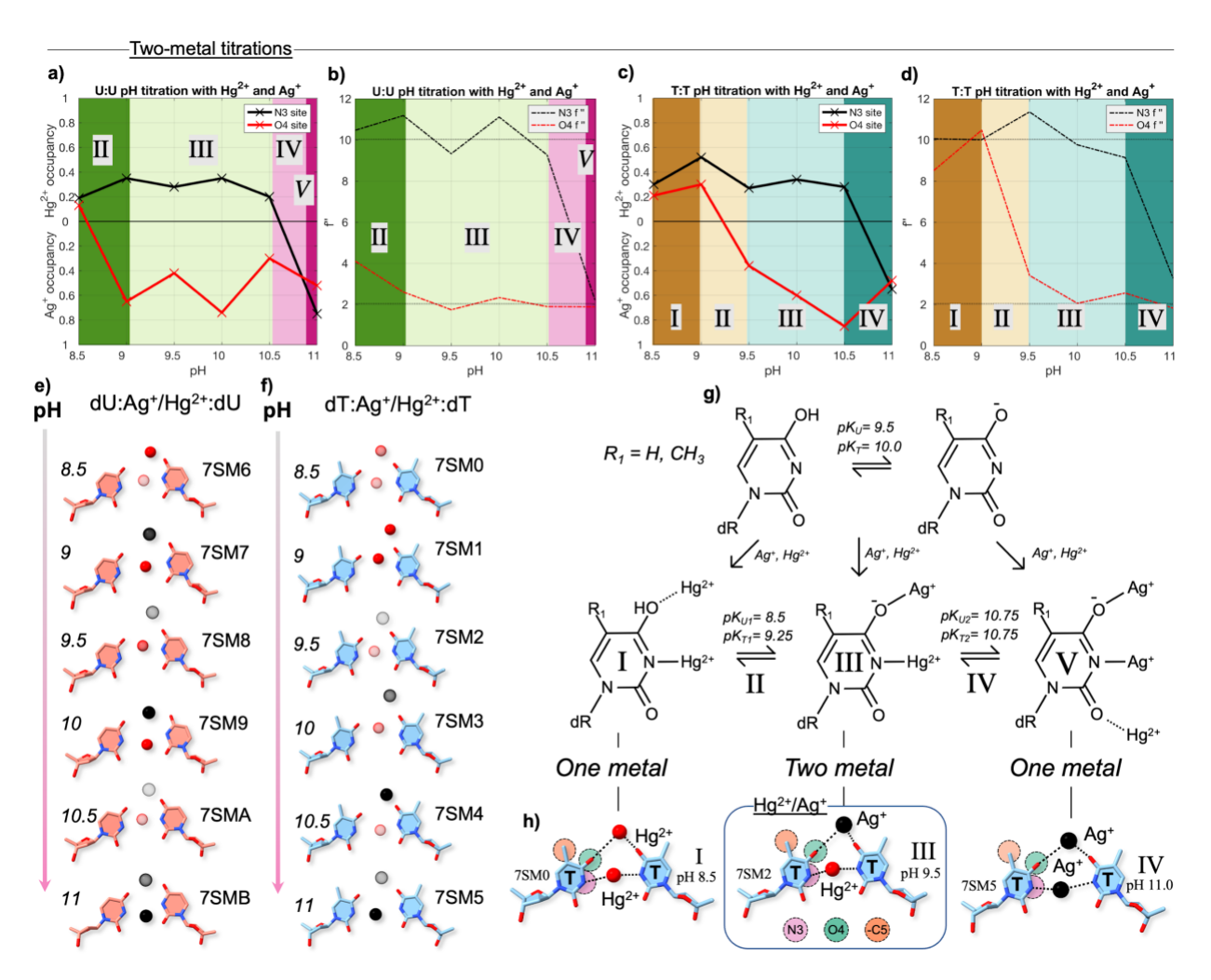


Figure 3: Crystallographic pH titrations for double metal (dT:Ag⁺/Hg²⁺:dT and dU:Ag⁺/Hg²⁺:dU) mmDNA base pairs in Tris buffer. **a-d)** Tandem chelation of is shown with dU:dU and dT:dT in the presence of both Ag⁺ and Hg²⁺. Occupancies are plotted for Hg²⁺ (positive y values) and Ag⁺ (negative y values). The shape of the occupancy curve matches the anomalous scattering f'' plot for each structure. Theoretical f'' values for Hg²⁺ and Ag⁺ at 12307 eV (10.17 and 2.06, respectively)³⁹ are displayed as horizontal lines. The reaction phases (I-V) are labeled. **e-f)** Crystal structures, PDB IDs and pH values are shown, with the transparency of each sphere (red and black for Hg²⁺ and Ag⁺, respectively) normalized for occupancy. **g)** A reaction scheme is derived from the crystallographic data which describes the structural changes across five phases (I-V), with II and IV being possible intermediates. **h)** Representative structures at pH 8.5, 9.5, and 11.0 are shown with pH 9.5 (boxed) containing both Hg²⁺ and Ag⁺.

It is widely accepted that the N3 position of uracil and thymine binds to mercury(II) ions. 9,10,18,33,40 This, combined with the tunability of silver(I) at the O4 position shown above, suggests the existence of an mmDNA base pair containing both silver (I) and mercury(II). We crystallized tensegrity triangles containing T-T (Figure S4) and U-U pairs (Figure S5) in a solution with both silver(I) and mercury(II) ions at pH levels of 8.5, 9.0, 9.5, 10.0, 10.5, and 11.0 (Figure 3). Structures were solved using anomalous dispersion at the measured mercury L_{III} edge (12307 eV) with resolutions of 3.3-4.8 Å. The heavy atoms were identified based on refined f" anomalous scattering factor values of each anomalous group and compared to the theoretical values at 12300 eV which are easily discernible at 2.06 for silver and 10.17 for mercury (Table S3-4).⁴¹ Electron density maps at this resolution are capable of distinguishing two distinct heavy atom sites (Figure S8) and f" anomalous scattering refinement clearly differentiates these sites from any spurious waters and magnesium ions due to 137-fold higher anomalous signal.⁴¹ We found that the N3 position binds to mercury(II) at pH 8.5-10.5 with little occupancy change, indicating the relative insensitivity of that site over that pH range (f" values and occupancies shown in Figure 3a-d; structures shown in Figure 3e-f).

However, at pH 11.0 for both thymine and uracil, we observed that the N3 position binds to silver(I) rather than mercury(II) based on f" values of that site. This could be related to the observation that the N3 position on thymine does not readily bind mercury(II) at pH 11.0 (Figure 2e). The f" value (3.29) of thymine's N3 silver(I) was slightly higher than expected (2.06), indicating the possibility of mercury(II) bound to a few units in the same crystal (Table S3), compared to uracil's N3 f" which was close to the expected value of 2.06 (Table S4). Because we previously found that uracil binds more silver(I) ions at the same pH value, we suspect that the threshold for silver(I) binding in uracil to be at a slightly lower pH than in thymine at the N3 position as well. In sum, the data showed that we have modified the behavior of thymine and uracil to bind silver(I) at both sites, similar to 4-thiothymine from a previous work. These results were unexpected as dT:Ag+:dT and dU:Ag+:dU (without mercury(II)) at pH 11.0 contain silver(I) exclusively at the O4 position. Given that the difference between these crystals was the addition of mercury(II), we believe that mercury(II) plays a role in increasing the silver binding propensity at the N3 position through the complete N3 deprotonation.

properties of the N3 position by weakly binding at the O2 site (**Figure 2e**, **Figure S9**). In dC:Ag⁺:dC, it has been hypothesized that silver(I) acts in the place of a proton to bind to the imine N3 position of cytosine.⁴³ Similarly, mercury(II) may stabilize the imine resonance structure of a deprotonated thymine and uracil by binding at the O2 site to enable the coordination of silver(I). As such, we propose a potential reaction scheme (**Figure 3g**) in which different pH conditions favor either the imine or amide structures which enable different metals to bind which captures the three representative structures (**Figure 3h**) in this pH range.

Heavy atom identity also varied based on the pH at the O4 position in the major groove in both thymine and uracil. With thymine, the O4 position changes from mercury(II) at pH 8.5 and 9.0 to silver(I) at pH 9.5 and above. In uracil, the same change occurs with mercury (II) at pH 8.5 and silver(I) at pH 9.0 and above. Additionally, we suspect a contribution from mercury(II) to the O4 position of thymine at pH 9.5 as the f'' values were much higher than expected. This phenomenon was not observed in uracil, showcasing the electronic effect of the methyl group at the 5-position in thymine. These findings indicate that local pH conditions enable the specific chelation of two different metal ions in the thymine and uracil base pairs. As such, we show fine control over three distinct modes of thymine and uracil coordination with silver(I) and mercury(II): $[Hg^{2+}/Hg^{2+}]$, $[Hg^{2+}/Ag^{+}]$, and $[Ag^{+}/Ag^{+}]$.

Tandem Chelation in Cytosine Base Pairs

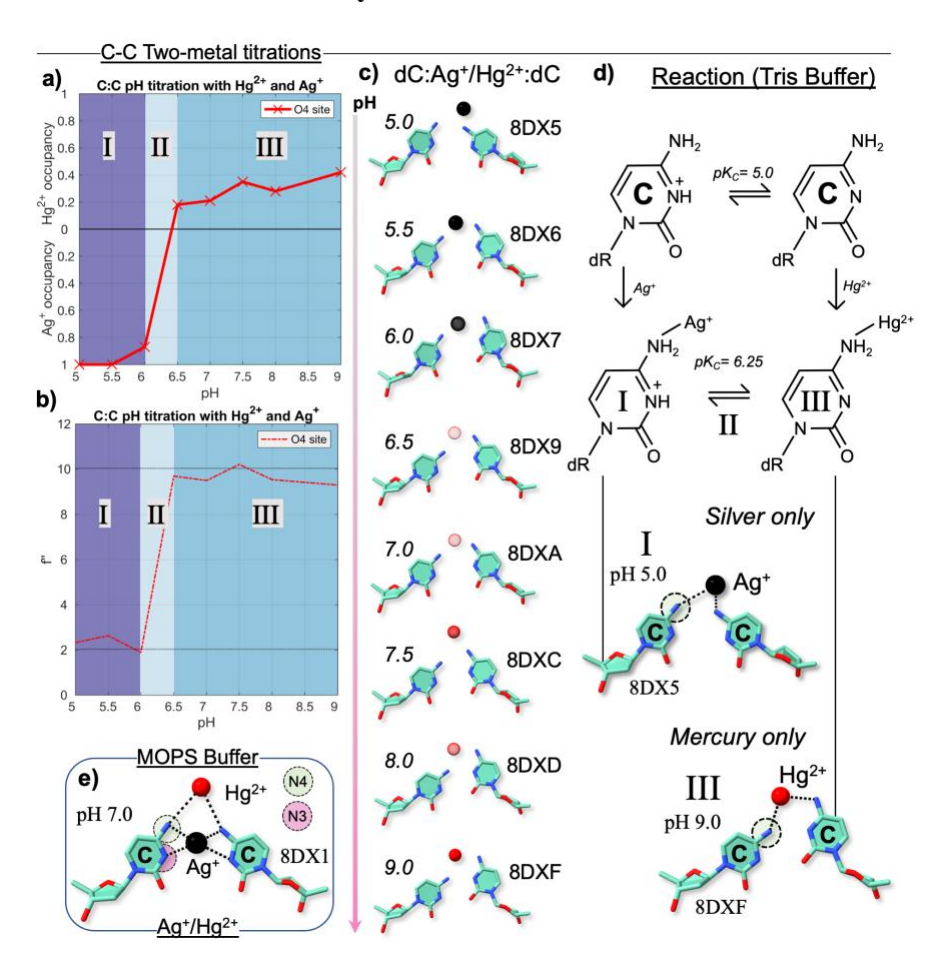


Figure 4: Crystallographic pH titrations for double metal dC:Ag⁺/Hg²⁺:dC mmDNA base pairs. **a-b)** dC:dC in the presence of Ag⁺ and Hg²⁺ with occupancies and f" values plotted. The reaction phases (I-III) are labeled. **c)** Crystal structures, PDB IDs and pH values are shown, with the transparency of each sphere (red and black for Hg²⁺ and Ag⁺, respectively) normalized for occupancy. **d)** Reaction scheme derived from the crystallographic data which describes the structural changes at pH 5.0 and 9.0 with representative structures shown. **e)** In contrast to the structures in Tris buffer (c-d), dC:dC chelates both metals in tandem in MOPS buffer at pH 7.0 (PDB ID: 8DX1).

We tested the pH-dependence of dC:Ag⁺/Hg²⁺:dC in MOPS and Tris and found no change from pH 6.0-8.0 in MOPS and clear evidence of pH-dependence in Tris (**Figure 4**). In Tris, we were able to exchange the metal bound at the N4 site with varying pH (occupancy and f'' values in **Figure 4a-b**, **Table S5**, structures in **Figure 4c**, and proposed reaction scheme in **Figure 4d**).

From pH 5.0-6.0, silver(I) binds with high occupancy; at pH 6.5 and above, mercury(II) binds with increasing occupancy. The pair dC:dC crystallized with mercury(II) does not contain any metals at pH 5.5 and 6.0 and does not crystallize in higher pH (Figure S6), which could indicate mercury(II) and silver(I) interacting in these structures to stabilize the observed mercury(II). In MOPS buffer, we found cytosine bases to be amenable to tandem chelation of silver(I) and mercury(II) (Figure 4e). Silver(I) binds at the N3 position (occ: 1.00, f''=2.73) and mercury(II) binds at the N4 position (occ: 0.58, f''=10.37) (Figure S10). This is the first example of two cytosine bases binding mercury(II) at any site and opens the door to the diversification of mmDNA binding modes across pH and buffer conditions more widely.

Alkaline pH-assisted Incorporation of Non-standard Metals

Since silver(I) can be found only at the O4 position at pH 11.0 without the presence of mercury(II) in solution (Figure 5a), while the addition of mercury(II) to the motifyielded the appearance of a second silver(I) at the N3 position (Figure 5b), we conclude that in crystals grown with both metals at high pH, mercury(II) can work as a "cofactor" to drive additional metal coordination in mmDNA. To explore the dual effects of alkaline pH and the presence of mercury(II), we tested additional combinations of metals with mercury(II) as a cofactor at pH 11.0 in dT:dT. We screened transition metals at pH 11.0 using the same conditions as dT:Ag⁺/Hg²⁺:dT above. Gold(I) in the presence of mercury(II) (Figure 5c) yielded an identical structure to gold(I) alone in a previous study, 9 indicating that mercury(II) does not participate in gold(I) incorporation (Figure 5d). We further found that dT:Hg²⁺/Hg²⁺:dT contains mercury(II) at both the O2 and O4 positions, not N3 (Figure 5e). Finally, we succeeded at incorporating cadmium(II) using mercury(II) as a cofactor at pH 11.0 (Figure 5f, Figure S7). dT:Hg²⁺/Cd²⁺:dT at pH 11.0 behaves in a similar manner as dT:Ag⁺/Hg²⁺:dT at pH 9.0-10.0, with mercury(II) in the N3 position (occ: 0.43, f''= 10.35) and cadmium(II) in the major groove O4 position (occ: 0.81, f''=2.35). Like silver(I), cadmium(II) has a vastly different f" value (2.25) at 12307 eV compared to mercury(II),39 which allows us to unequivocally confirm the presence of cadmium in this structure.

Alkaline pH Effects on Metal and Hetero-Metal Pairs ---pH 11.0 Single Metal ---- pH 11.0 Hetero-metal ---a) b) 7SLG AgNO3, HgCl2 Crystallized w/ c) d) **7UL8** Cd24 Hg²⁺ f) e) CdSO (O2) (N3) (O4) h)

Figure 5: Alkaline pH and hetero-metal effects on metal-mediated DNA base pairing in Tris buffer. **a-f)** mmDNA base pairs with single metals compared to results with additional metals. Of note, Hg²⁺ with Ag⁺ results in two bound Ag⁺ ions (7SM5); and Hg²⁺ with Cd²⁺ result in a novel cadmium(II) base pair (7UJZ); while Au⁺ is unaffected by HgCl₂ (7UK0). **g)** View of dT:Hg²⁺/Cd²⁺:dT at pH 11.0. **h)** Composite overlay of various pH 11.0 structures indicates considerable isomorphism between T-T base pair motifs.

Cadmium(II) is thought to have similar coordination behavior as mercury(II),⁴⁴ but we do not observe this characteristic in our DNA complex. Instead, cadmium(II) behaves in a similar manner as silver(I) and gold(I) in our system. As such, we hypothesize that it may be possible to replace the N3 mercury(II) with cadmium(II) at pH values above 11.0. We further tested our method on gold(III) and found that it may be possible to incorporate gold(III) at the N3 position (**Figure S12**, **Table S6**), but results are not conclusive enough for us to assign the N3 ion as gold(III) and not mercury(II). Overall, we determined that alkaline pH assists in the formation of two novel mmDNA base pairs and should be studied in further detail for additional metal incorporation. The

definite impact of mercury(II) requires additional screening to further expand the semantomorphic alphabet of possible mmDNA base pairs.

Conclusions

Using the tensegrity triangle motif as a scaffold to drive B-form crystallization allowed us to develop a method of taking crystallographic snapshots for the structure determination of mmDNA base pairs. Motifs containing dT:Ag⁺:dT and dU:Ag⁺:dU show strong pH dependence, titrating from a crystallographic occupancy of 0.0 to 1.0 for a pH range of 8.0-10.0. Using this pH-dependent binding site, we further determined the structures of mmDNA homothymine and homouracil base pairs with silver(I) at the O4 position and mercury(II) at the N3 position and analyzed their behavior across pH values of 8.5-11.0, discovering three pH-dependent binding modes with tandem chelation of mercury(II) and silver(I). We additionally tested this method on cytosine and identified the pH-dependent incorporation of mercury(II) into homocytosine base pairs as well as a heterometal base pair with both silver(I) and mercury(II).

In this way, structural 3D DNA nanotechnology and x-ray crystallography allowed us to produce very comprehensive observations of the behavior of T-T, U-U, and C-C bases in the presence of transition metal ions. We believe that enhanced understanding of mmDNA base pairing will contribute to the design and self-assembly of DNA architectures based on the unique electronic properties and reactivity of these base pairs as well as introduce new methods for more complete analysis of different modes of DNA base pairing. The existence of heterometal base pairs and their highly specific environmental requirements provides an exciting foothold for tunable topological nanowires. 12,45 As such, future physical studies of mmDNA should include heterometal base pairs, which greatly diversify the DNA chemical design language. Furthermore, considerable attention has been given to the electronic properties of silver(I) base pairs at neutral pH. ^{39,43} The ability of unmodified DNA bases to capture ions of gold and cadmium will necessitate the expanded study of DNA nanoelectronics. It is also clear that further studies on metal coordination that exploit alkaline pH and mercury(II) as a cofactor will further diversify mmDNA toward heterometallic wires and devices. We anticipate future mmDNA motifs to make use of these results for pH sensitive nanodevices, 46-48 catalytic oligonucleotides, 49,50 reaction centers, 13 sensing platforms, 40 and molecular computing.⁵¹

Acknowledgments

Results shown in this report are derived from work performed at Argonne National Laboratory, Structural Biology Center (SBC) at the Advanced Photon Source. SBC-CAT is operated by UChicago Argonne, LLC, for the U.S. Department of Energy, Office of Biological and Environmental Research under contract DE-AC02-06CH11357. This research used resources of the Advanced Photon Source, a U.S. Department of Energy (DOE) Office of Science User Facility operated for the DOE Office of Science by Argonne National Laboratory under Contract No. DE-AC02-06CH11357. This research used resources at the Industrial Macromolecular Crystallography Association Collaborative Access Team (IMCA-CAT) beamline 17-ID, supported by the companies of the Industrial Macromolecular Crystallography Association through a contract with Hauptman-Woodward Medical Research Institute. We thank A. Mulichak, E. Zoellner, and J. Digilio at IMCA-CAT for their assistance with diffraction experiments. Funding: We acknowledge support of grants N000141912596 from the Office of Naval Research, DE-SC0007991 from the Department of Energy, 2106790 from the National Science Foundation, RPG0010/2017 from Human Frontiers Science Program, DMR-1420073 from the MRSEC Program of the National Science Foundation, and the 2020 NASA Center Innovation Fund (CIF) Program. Author Contributions: B.L. devised the project, grew the crystals, collected data, analyzed data, and wrote the paper; Y.P.O. devised the motif, guided the project, and wrote the paper; R.S. guided the project and wrote the paper. K.W. collected the data and analyzed the data; J. Y. devised the collection strategy and analyzed data; C.Y. synthesized the soluble Au(I) ligand. L.J.R. analyzed data, and wrote the paper; S.J.W. analyzed data, and wrote the paper; W.A.H. devised the collection and refinement strategy; J.W.C. analyzed the data and wrote the paper. C.M. devised the motif and wrote the paper; N.C.S. initiated and guided the project, analyzed data and wrote the paper. S.V. initiated and guided the project, grew crystals, collected data, analyzed data, and wrote the paper. Competing interests: The authors claim no competing interests. Data availability: Atomic coordinates and experimental structure factors have been deposited within the Protein Data Bank and are accessible under PDB IDs: 7SLB-7SLG, 7SLJ-7SLO, 7SM0-7SMB, 7TI3, 7UJZ, 7UK0, and 8DXV-8DXZ. Any additional information required to reanalyze the data reported in this paper is available upon request.

References

- Lu, B., Vecchioni, S., Ohayon, Y. P., Sha, R., Woloszyn, K., Yang, B., Mao, C. & Seeman, N. C. 3d Hexagonal Arrangement of DNA Tensegrity Triangles. *ACS Nano* 15, 16788-16793, doi:10.1021/acsnano.1c06963 (2021).
- Zheng, J., Birktoft, J. J., Chen, Y., Wang, T., Sha, R., Constantinou, P. E., Ginell, S. L., Mao, C. & Seeman, N. C. From Molecular to Macroscopic Via the Rational Design of a Self-Assembled 3d DNA Crystal. *Nature* **461**, 74-77, doi:10.1038/nature08274 (2009).
- Mao, C., Sun, W., Shen, Z. & Seeman, N. C. A Nanomechanical Device Based on the B-Z Transition of DNA. *Nature* **397**, 144-146, doi:10.1038/16437 (1999).
- Chen, J. H. & Seeman, N. C. Synthesis from DNA of a Molecule with the Connectivity of a Cube. *Nature* **350**, 631-633, doi:10.1038/350631a0 (1991).
- 5 Seeman, N. C. Nucleic Acid Junctions and Lattices. *J Theor Biol* **99**, 237-247, doi:10.1016/0022-5193(82)90002-9 (1982).
- Zhang, C., Zhao, J., Lu, B., Seeman, N. C., Sha, R., Noinaj, N. & Mao, C. Engineering DNA Crystals toward Studying DNA-Guest Molecule Interactions. *J. Am. Chem. Soc.* **145**, 4853-4859, doi:10.1021/jacs.3c00081 (2023).
- Zhao, J., Zhang, C., Lu, B., Sha, R., Noinaj, N. & Mao, C. Divergence and Convergence: Complexity Emerges in Crystal Engineering from an 8-Mer DNA. *J. Am. Chem. Soc.* **145**, 10475-10479, doi:10.1021/jacs.3c01941 (2023).
- Hoshika, S., Leal, N. A., Kim, M. J., Kim, M. S., Karalkar, N. B., Kim, H. J., Bates, A. M., Watkins, N. E., Jr., SantaLucia, H. A., Meyer, A. J., DasGupta, S., Piccirilli, J. A., Ellington, A. D., SantaLucia, J., Jr., Georgiadis, M. M. & Benner, S. A. Hachimoji DNA and Rna: A Genetic System with Eight Building Blocks. *Science* **363**, 884-887, doi:10.1126/science.aat0971 (2019).
- Vecchioni, S., Lu, B., Livernois, W., Ohayon, Y. P., Yoder, J., Yang, C., Woloszyn, K., Bernfield, W., Anantram, M. P., Canary, J. W., Hendrickson, W. A., Rothschild, L. J., Mao, C., Wind, S. J., Seeman, N. C. & Sha, R. Metal-Mediated DNA Nanotechnology in 3d: Structural Library by Templated Diffraction. *Adv Mater*, e2210938, doi:10.1002/adma.202210938 (2023).
- Miyake, Y., Togashi, H., Tashiro, M., Yamaguchi, H., Oda, S., Kudo, M., Tanaka, Y., Kondo, Y., Sawa, R., Fujimoto, T., Machinami, T. & Ono, A. Mercuryii-Mediated Formation of Thymine-Hgii-Thymine Base Pairs in DNA Duplexes. *J. Am. Chem. Soc.* **128**, 2172-2173, doi:10.1021/ja056354d (2006).
- Dairaku, T., Furuita, K., Sato, H., Sebera, J., Nakashima, K., Kondo, J., Yamanaka, D., Kondo, Y., Okamoto, I., Ono, A., Sychrovsky, V., Kojima, C. & Tanaka, Y. Structure Determination of an Ag(I) -Mediated Cytosine-Cytosine Base Pair within DNA Duplex in Solution with (1) H/(15) N/(109) Ag Nmr Spectroscopy. *Chemistry* 22, 13028-13031, doi:10.1002/chem.201603048 (2016).
- Vecchioni, S., Capece, M. C., Toomey, E., Nguyen, L., Ray, A., Greenberg, A., Fujishima, K., Urbina, J., Paulino-Lima, I. G., Pinheiro, V., Shih, J., Wessel, G., Wind, S. J. & Rothschild, L. Construction and Characterization of Metal Ion-Containing DNA Nanowires for Synthetic Biology and Nanotechnology. *Sci Rep* 9, 6942, doi:10.1038/s41598-019-43316-1 (2019).

- Dairaku, T., Kawai, R., Kanaba, T., Ono, T., Yoshida, K., Sato, H., Nozawa-Kumada, K., Kondo, Y., Kondo, J., Ono, A., Tanaka, Y. & Kashiwagi, Y. Effect of Cytosine-Ag(+)-Cytosine Base Pairing on the Redox Potential of the Ag(+)/Ag Couple and the Chemical Reduction of Ag(+) to Ag by Tetrathiafulvalene. *Dalton Trans* **50**, 7633-7639, doi:10.1039/d1dt00975c (2021).
- Mandal, S. & Muller, J. Metal-Mediated DNA Assembly with Ligand-Based Nucleosides. *Curr Opin Chem Biol* **37**, 71-79, doi:10.1016/j.cbpa.2017.01.019 (2017).
- Kondo, J., Tada, Y., Dairaku, T., Hattori, Y., Saneyoshi, H., Ono, A. & Tanaka, Y. A Metallo-DNA Nanowire with Uninterrupted One-Dimensional Silver Array. *Nat Chem* **9**, 956-960, doi:10.1038/nchem.2808 (2017).
- Kondo, J., Sugawara, T., Saneyoshi, H. & Ono, A. Crystal Structure of a DNA Duplex Containing Four Ag(I) Ions in Consecutive Dinuclear Ag(I)-Mediated Base Pairs: 4-Thiothymine-2ag(I)-4-Thiothymine. *Chem Commun (Camb)* **53**, 11747-11750, doi:10.1039/c7cc06153f (2017).
- Yamaguchi, H., Sebera, J., Kondo, J., Oda, S., Komuro, T., Kawamura, T., Dairaku, T., Kondo, Y., Okamoto, I., Ono, A., Burda, J. V., Kojima, C., Sychrovsky, V. & Tanaka, Y. The Structure of Metallo-DNA with Consecutive Thymine-Hgii-Thymine Base Pairs Explains Positive Entropy for the Metallo Base Pair Formation. *Nucleic Acids Res* **42**, 4094-4099, doi:10.1093/nar/gkt1344 (2014).
- 18 Kondo, J., Yamada, T., Hirose, C., Okamoto, I., Tanaka, Y. & Ono, A. Crystal Structure of Metallo DNA Duplex Containing Consecutive Watson-Crick-Like T-Hgii-T Base Pairs. *Angew. Chem.* **126**, 2417-2420, doi:10.1002/ange.201309066 (2014).
- Ennifar, E., Walter, P. & Dumas, P. A Crystallographic Study of the Binding of 13 Metal Ions to Two Related Rna Duplexes. *Nucleic Acids Res* **31**, 2671-2682, doi:10.1093/nar/gkg350 (2003).
- Lei, P., Li, Y., Song, X., Hao, Y. & Deng, Z. DNA-Programmable Agaus-Primed Conductive Nanowelding Wires-up Wet Colloids. *Angew. Chem.* **134**, doi:10.1002/ange.202203568 (2022).
- 21 Xing, X., Feng, Y., Yu, Z., Hidaka, K., Liu, F., Ono, A., Sugiyama, H. & Endo, M. Direct Observation of the Double-Stranded DNA Formation through Metal Ion-Mediated Base Pairing in the Nanoscale Structure. *Chemistry* **25**, 1446-1450, doi:10.1002/chem.201805394 (2019).
- Takezawa, Y., Suzuki, A., Nakaya, M., Nishiyama, K. & Shionoya, M. Metal-Dependent DNA Base Pairing of 5-Carboxyuracil with Itself and All Four Canonical Nucleobases. *J. Am. Chem. Soc.* **142**, 21640-21644, doi:10.1021/jacs.0c11437 (2020).
- Schmidt, O. P., Jurt, S., Johannsen, S., Karimi, A., Sigel, R. K. O. & Luedtke, N. W. Concerted Dynamics of Metallo-Base Pairs in an a/B-Form Helical Transition. *Nat Commun* **10**, 4818, doi:10.1038/s41467-019-12440-x (2019).
- Ono, A., Kanazawa, H., Ito, H., Goto, M., Nakamura, K., Saneyoshi, H. & Kondo, J. A Novel DNA Helical Wire Containing Hg(Ii) -Mediated T:T and T:G Pairs. *Angew. Chem. Int. Ed.* **58**, 16835-16838, doi:10.1002/anie.201910029 (2019).
- Atsugi, T., Ono, A., Tasaka, M., Eguchi, N., Fujiwara, S. & Kondo, J. A Novel Ag(I) DNA Rod Comprising a One-Dimensional Array of 11 Silver Ions within a Double Helical Structure. *Angew. Chem. Int. Ed.* **61**, e202204798, doi:10.1002/anie.202204798 (2022).

- Ohayon, Y. P., Hernandez, C., Chandrasekaran, A. R., Wang, X., Abdallah, H. O., Jong, M. A., Mohsen, M. G., Sha, R., Birktoft, J. J., Lukeman, P. S., Chaikin, P. M., Ginell, S. L., Mao, C. & Seeman, N. C. Designing Higher Resolution Self-Assembled 3d DNA Crystals Via Strand Terminus Modifications. *ACS Nano* 13, 7957-7965, doi:10.1021/acsnano.9b02430 (2019).
- Lu, B., Vecchioni, S., Ohayon, Y. P., Canary, J. W. & Sha, R. The Wending Rhombus: Self-Assembling 3d DNA Crystals. *Biophys J* **121**, 4759-4765, doi:10.1016/j.bpj.2022.08.019 (2022).
- Woloszyn, K., Vecchioni, S., Ohayon, Y. P., Lu, B., Ma, Y., Huang, Q., Zhu, E., Chernovolenko, D., Markus, T., Jonoska, N., Mao, C., Seeman, N. C. & Sha, R. Augmented DNA Nanoarchitectures: A Structural Library of 3d Self-Assembling Tensegrity Triangle Variants. *Adv Mater* **34**, e2206876, doi:10.1002/adma.202206876 (2022).
- Lu, B., Woloszyn, K., Ohayon, Y. P., Yang, B., Zhang, C., Mao, C., Seeman, N. C., Vecchioni, S. & Sha, R. Programmable 3d Hexagonal Geometry of DNA Tensegrity Triangles. *Angew. Chem. Int. Ed.* **62**, e202213451, doi:10.1002/anie.202213451 (2023).
- Lu, B., Vecchioni, S., Ohayon, Y. P., Woloszyn, K., Markus, T., Mao, C., Seeman, N. C., Canary, J. W. & Sha, R. Highly Symmetric, Self-Assembling 3d DNA Crystals with Cubic and Trigonal Lattices. *Small* 19, e2205830, doi:10.1002/smll.202205830 (2023).
- Vecchioni, S., Lu, B., Janowski, J., Woloszyn, K., Jonoska, N., Seeman, N. C., Mao, C., Ohayon, Y. P. & Sha, R. The Rule of Thirds: Controlling Junction Chirality and Polarity in 3d DNA Tiles. *Small* **19**, e2206511, doi:10.1002/smll.202206511 (2023).
- Furukawa, A., Walinda, E., Arita, K. & Sugase, K. Structural Dynamics of Double-Stranded DNA with Epigenome Modification. *Nucleic Acids Res* **49**, 1152-1162, doi:10.1093/nar/gkaa1210 (2021).
- Okamoto, I., Iwamoto, K., Watanabe, Y., Miyake, Y. & Ono, A. Metal-Ion Selectivity of Chemically Modified Uracil Pairs in DNA Duplexes. *Angew. Chem. Int. Ed.* **48**, 1648-1651, doi:10.1002/anie.200804952 (2009).
- Krishnamurthy, R. Role of Pk(a) of Nucleobases in the Origins of Chemical Evolution. *Acc Chem Res* **45**, 2035-2044, doi:10.1021/ar200262x (2012).
- Ganguly, S. & Kundu, K. K. Protonation/Deprotonation Energetics of Uracil, Thymine, and Cytosine in Water from E.M.F./Spectrophotometric Measurements. *Canadian Journal of Chemistry* **72**, 1120-1126, doi:10.1139/v94-143 (1994).
- Sebera, J., Burda, J., Straka, M., Ono, A., Kojima, C., Tanaka, Y. & Sychrovsky, V. Formation of a Thymine-Hg(Ii)-Thymine Metal-Mediated DNA Base Pair: Proposal and Theoretical Calculation of the Reaction Pathway. *Chemistry* **19**, 9884-9894, doi:10.1002/chem.201300460 (2013).
- Nishiyama, K., Takezawa, Y. & Shionoya, M. Ph-Dependence of the Thermal Stability of Metallo-DNA Duplexes Containing Ligand-Type 5-Hydroxyuracil Nucleobases. *Inorganica Chimica Acta* **452**, 176-180, doi:10.1016/j.ica.2016.04.040 (2016).
- Wincel, H. Microhydration of Deprotonated Nucleobases. *J Am Soc Mass Spectrom* **27**, 1383-1392, doi:10.1007/s13361-016-1411-3 (2016).
- Cromer, D. T. & Waber, J. T. Scattering Factors Computed from Relativistic Dirac–Slater Wave Functions. *Acta Crystallogr.* **18**, 104-109, doi:10.1107/s0365110x6500018x (1965).

- Wang, Z., Heon Lee, J. & Lu, Y. Highly Sensitive "Turn-on" Fluorescent Sensor for Hg2+ in Aqueous Solution Based on Structure-Switching DNA. *Chem Commun (Camb)*, 6005-6007, doi:10.1039/b812755g (2008).
- Liu, Q., Liu, Q. & Hendrickson, W. A. Robust Structural Analysis of Native Biological Macromolecules from Multi-Crystal Anomalous Diffraction Data. *Acta Crystallogr. D* **69**, 1314-1332, doi:10.1107/S0907444913001479 (2013).
- Torigoe, H., Ono, A. & Kozasa, T. Hg(Ii) Ion Specifically Binds with T:T Mismatched Base Pair in Duplex DNA. *Chemistry* **16**, 13218-13225, doi:10.1002/chem.201001171 (2010).
- Fardian-Melamed, N., Katrivas, L., Eidelshtein, G., Rotem, D., Kotlyar, A. & Porath, D. Electronic Level Structure of Silver-Intercalated Cytosine Nanowires. *Nano Lett* **20**, 4505-4511, doi:10.1021/acs.nanolett.0c01292 (2020).
- Borsari, M. in *Encyclopedia of Inorganic and Bioinorganic Chemistry* 1-16 (2014).
- Zhou, H., Lin, H., Wang, Q., Hao, T., Hu, Y., Wang, S. & Guo, Z. Tunneling or Hopping? A Direct Electrochemical Observation of Electron Transfer in DNA. *Anal Chem* **94**, 15324-15331, doi:10.1021/acs.analchem.2c02794 (2022).
- Hao, Y., Kristiansen, M., Sha, R., Birktoft, J. J., Hernandez, C., Mao, C. & Seeman, N.
 C. A Device That Operates within a Self-Assembled 3d DNA Crystal. *Nat Chem* 9, 824-827, doi:10.1038/nchem.2745 (2017).
- 47 Mattath, M. N., Ghosh, D., Pratihar, S., Shi, S. & Govindaraju, T. Nucleic Acid Architectonics for Ph-Responsive DNA Systems and Devices. *ACS Omega* 7, 3167-3176, doi:10.1021/acsomega.1c06464 (2022).
- Zheng, L. L., Li, J. Z., Li, Y. X., Gao, J. B., Dong, J. X. & Gao, Z. F. Ph-Responsive DNA Motif: From Rational Design to Analytical Applications. *Front Chem* **9**, 732770, doi:10.3389/fchem.2021.732770 (2021).
- Lippert, B. Ligand-Pka Shifts through Metals: Potential Relevance to Ribozyme Chemistry. *Chem Biodivers* **5**, 1455-1474, doi:10.1002/cbdv.200890135 (2008).
- Borggrafe, J., Victor, J., Rosenbach, H., Viegas, A., Gertzen, C. G. W., Wuebben, C., Kovacs, H., Gopalswamy, M., Riesner, D., Steger, G., Schiemann, O., Gohlke, H., Span, I. & Etzkorn, M. Time-Resolved Structural Analysis of an Rna-Cleaving DNA Catalyst. *Nature* **601**, 144-149, doi:10.1038/s41586-021-04225-4 (2021).
- Robinson, B. H. & Seeman, N. C. The Design of a Biochip: A Self-Assembling Molecular-Scale Memory Device. *Protein Eng* **1**, 295-300, doi:10.1093/protein/1.4.295 (1987).